Supporting Information: Exploring non-covalent interactions in excited states: beyond aromatic excimer models

Ariel C. Jones and Lars Goerigk*

School of Chemistry, The University of Melbourne, Parkville, Australia;

Ph: +61-3-83446784

E-mail: lars.goerigk@unimelb.edu.au

Contents

1 Details for CBS extrapolation

A TZ-QZ CBS extrapolation was performed to obtain the final SCS-CC2/CBS(3,4) reference energies. As outlined before by our group,[S1] CCS total energies were used as the component of the total excited state energy that does not include electron correlation. The correlation energy is the difference between the CCS total energy and the SCS-CC2 total energy for a given excited state. The equations for the extrapolations are shown in Equation 1 for CCS total energy[S2] and Equation 2 for correlation energy.[S3] Here, X and Y represent successive cardinal numbers (3 and 4 for a TZ-QZ extrapolation). For the Ahlrichs basis set and TZ-QZ extrapolation, $\alpha = 7.88$ and $\beta = 2.97$.[S4]

$$E_{CCS} = \frac{E_{CCS}^{(X)} \cdot exp(-\alpha\sqrt{Y}) - E_{CCS}^{(Y)} \cdot exp(-\alpha\sqrt{X})}{exp(-\alpha\sqrt{Y}) - exp(-\alpha\sqrt{X})} \tag{1}$$

$$E_{Corr} = \frac{X^{\beta} \cdot E_c^{(X)} - Y^{\beta} \cdot E_c^{(Y)}}{X^{\beta} - Y^{\beta}} \tag{2}$$

Hancock and Goerigk showed that SCS-CC2/CBS(3,4) was a suitably accurate reference method for aromatic excimers.[S1] We also show good accuracy for SCS-CC2/CBS(3,4) in the context of exciplexes by comparing against interaction energies calculated at the CCSDR(3)[S5]/def2-TZVP level of theory. CCSDR(3) can be considered as the excited-state analogue to CCSD(T), which provides highly accurate excited state energies. We calculated interaction energies for a select number of points on the benzene-neon exciplex dissociation curve, as shown in Figure S1. By interpolating between points, we find that CCSDR(3) gives a D_e of 0.35 kcal mol^{-1} which differs by only 0.06 kcal mol^{-1} compared to SCS-CC2/CBS(3,4). This small error justifies the use of SCS-CC2/CBS(3,4), which is feasible for the calculation of the larger exciplexes whereas CCSDR(3) becomes prohibitively expensive.

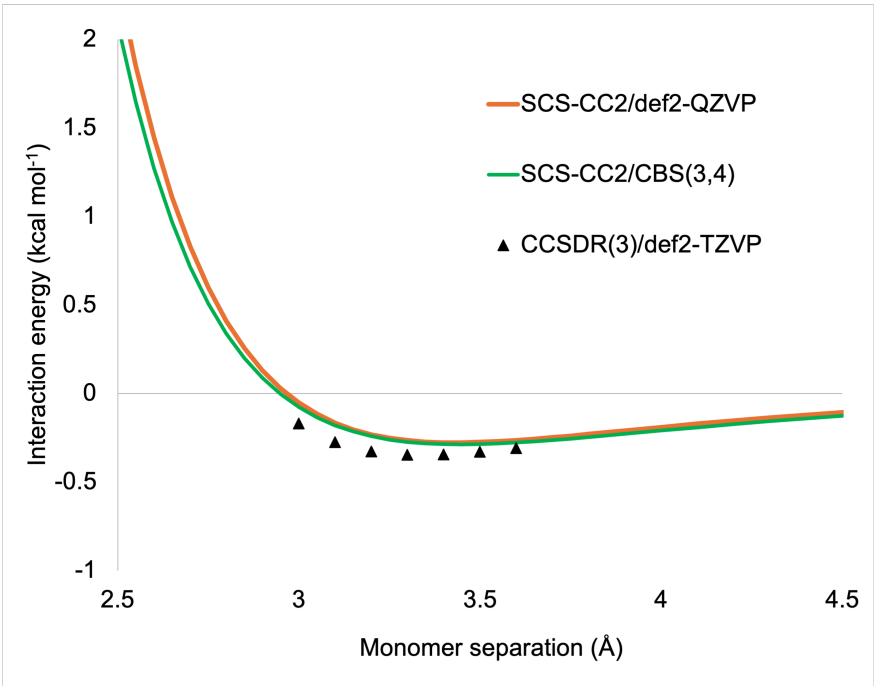

Figure S1: Dissociation curves for the benzene-neon exciplex calculated with SCS-CC2/def2-QZVP, SCS-CC2/CBS(3,4), and CCSDR(3)/def2-TZVP.

2 Values for D_e and r_e

Table S1: Benchmarking results for exciplexes with a localised excitation. Dissociation energies (D_e, kcal mol^{-1}) and equilibrium distances (r_e, Å) for TD-DFT methods are shown along with the SCS-CC2/CBS(3,4) reference. Where the D3(BJ) correction is available for a method, the dispersion-corrected value is shown in parentheses. Values of r_e are not reported for methods that produce an entirely repulsive dissociation curve (negative D_e).

Method	Benzene-neon		Benzene-argon		Benzene-anthracene		Toluene-TCNE 3A'	
	D_e	r_e	D_e	r_e	D_e	r_e	D_e	r_e
Reference	0.29	3.44	1.07	3.49	7.79	3.35	12.37	3.26
BLYP	-0.38(0.26)	(3.34)	-1.12(1.10)	(3.49)	-6.52(7.82)	(3.36)	1.20(11.65)	3.95(3.52)
BP86	-0.64(-0.04)		-1.09(1.02)	(3.46)	-4.55(9.17)	(3.29)	1.62(12.19)	3.73(3.52)
PBE	0.26(0.66)	3.48(3.26)	0.31(1.27)	3.90(3.53)	0.28(6.19)	4.20(3.44)	4.39(10.56)	3.67(3.55)
B97M-V	0.54	3.13	1.26	3.44	6.39	3.46	—[a]	—[a]
BHLYP	0.00(0.48)	3.54(3.19)	-0.03(1.16)	4.04(3.47)	-4.02(5.70)	(3.47)	3.66(11.58)	3.69(3.37)
B3LYP	-0.19(0.37)	(3.27)	-0.69(1.17)	(3.48)	-5.13(7.03)	(3.41)	2.93(13.50)	3.76(3.30)
PBE0	0.17(0.55)	3.50(3.29)	0.24(1.24)	3.90(3.53)	0.09(6.29)	4.20(3.45)	5.20(12.52)	3.52(3.30)
CAM-B3LYP	0.10(0.53)	3.36(3.20)	0.08(1.20)	3.85(3.52)	-0.32(6.13)	4.23(3.51)	4.24(11.35)	3.61(3.40)
LC-BLYP	0.99	2.92	1.04	3.37	1.96	3.57	8.49	3.35
LC-PBE	0.07	3.45	0.18	3.73	0.45	3.61	6.84	3.32
ωB97X	0.40	3.26	1.17	3.44	3.75	3.56	9.43	3.46
ωB97X-D3(BJ)	0.11(0.53)	3.54(3.22)	0.19(1.28)	3.89(3.42)	0.12(6.27)	4.01(3.40)	4.50(12.07)	3.67(3.32)
ωB97X-V	0.70	3.16	1.33	3.47	6.22	3.51	11.42	3.39
ωB97M-V	0.66	3.17	1.32	3.41	6.75	3.44	11.95	3.34
B2GP-PLYP	0.14(0.36)	3.37(3.27)	0.51(1.16)	3.59(3.45)	3.27(7.15)	3.56(3.39)	8.44(12.65)	3.39(3.29)
SCS-B2GP-PLYP	0.07(0.36)	3.54(3.23)	0.26(1.02)	3.76(3.45)	1.64(6.14)	3.72(3.40)	6.34(12.11)	3.51(3.26)
SOS-B2GP-PLYP	0.07(0.35)	3.54(3.24)	0.26(1.01)	3.76(3.45)	1.64(6.08)	3.72(3.40)	6.35(12.00)	3.51(3.27)
B2PLYP	0.06(0.36)	3.54(3.27)	0.27(1.17)	3.71(3.47)	1.97(7.34)	3.68(3.40)	6.89(12.86)	3.45(3.29)
SOS-B2PLYP	0.00(0.34)	3.81(3.24)	0.09(1.00)	4.02(3.44)	0.61(6.03)	3.94(3.38)	4.90(12.18)	3.59(3.24)
PBE-QIDH	0.20(0.31)	3.43(3.41)	0.64(1.03)	3.56(3.48)	3.88(6.54)	3.47(3.40)	9.64(12.06)	3.31(3.28)
SCS-PBE-QIDH	0.19(0.33)	3.44(3.41)	0.57(0.94)	3.62(3.53)	3.43(6.34)	3.50(3.42)	9.04(11.68)	3.32(3.29)
SOS-PBE-QIDH	0.17(0.34)	3.45(3.40)	0.53(0.95)	3.65(3.53)	3.12(6.37)	3.53(3.42)	8.65(11.70)	3.34(3.30)
PBE0-DH	0.16(0.43)	3.46(3.33)	0.38(1.20)	3.75(3.42)	1.38(6.54)	3.68(3.38)	6.86(12.63)	3.41(3.26)
RSX-0DH	0.09(0.14)	3.43(3.43)	0.39(0.63)	3.42(3.42)	1.98(3.74)	3.46(3.44)	8.59(9.98)	3.28(3.27)
RSX-QIDH	0.17(0.19)	3.38(3.38)	0.74(0.78)	3.39(3.39)	4.53(4.94)	3.36(3.36)	11.02(11.32)	3.23(3.23)
SCS-RSX-QIDH	0.22(0.22)	3.22(3.22)	0.94(0.94)	3.34(3.34)	5.79(5.83)	3.29(3.29)	12.54(12.56)	3.17(3.17)
SOS-RSX-QIDH	0.18(0.20)	3.38(3.38)	0.74(0.77)	3.38(3.38)	4.70(5.14)	3.35(3.34)	11.25(11.57)	3.21(3.21)
ωB2GP-PLYP	0.62(0.62)	3.04(3.04)	1.22(1.22)	3.37(3.37)	5.25(5.26)	3.42(3.42)	11.59(11.6)	3.29(3.29)
SCS-ωB2GP-PLYP	0.56(0.62)	3.07(3.07)	1.05(1.17)	3.41(3.40)	4.32(5.55)	3.47(3.45)	10.50(11.49)	3.32(3.31)
SOS-ωB2GP-PLYP	0.55(0.61)	3.07(3.07)	1.02(1.15)	3.42(3.41)	4.21(5.45)	3.48(3.46)	10.35(11.35)	3.32(3.32)
ωB2PLYP	0.67(0.68)	3.02(3.02)	1.15(1.16)	3.38(3.38)	4.32(4.54)	3.46(3.46)	10.72(10.87)	3.31(3.31)
SOS-ωB2PLYP	0.62(0.68)	3.03(3.03)	0.99(1.23)	3.41(3.40)	3.60(5.26)	3.50(3.47)	9.83(11.23)	3.33(3.32)
ωB88PP86	0.43(0.43)	3.06(3.06)	1.51(1.51)	3.26(3.26)	8.06(8.06)	3.25(3.25)	15.07(15.07)	3.14(3.14)
SCS-ωB88PP86	0.29(0.29)	3.15(3.15)	1.03(1.04)	3.34(3.34)	5.27(5.40)	3.36(3.36)	11.83(11.92)	3.23(3.23)
SOS-ωB88PP86	0.28(0.29)	3.15(3.15)	1.01(1.02)	3.34(3.34)	5.23(5.33)	3.36(3.36)	11.80(11.87)	3.23(3.23)
ωPBEPP86	0.61(0.61)	2.95(2.95)	2.01(2.01)	3.16(3.16)	10.63(10.63)	3.16(3.16)	18.30(18.0)	3.06(3.06)
SCS-ωPBEPP86	0.40(0.40)	3.04(3.04)	1.39(1.39)	3.26(3.26)	6.95(6.96)	3.28(3.28)	14.15(14.16)	3.16(3.16)
SOS-ωPBEPP86	0.39(0.39)	3.04(3.04)	1.32(1.32)	3.27(3.27)	6.69(6.69)	3.29(3.29)	13.83(13.83)	3.16(3.16)

[a] Did not give the correct dissociation limit, see main aticle.

Table S2: Benchmarking results for exciplexes with a CT excitation.

	Toluene-TCNE 2A'		Styrene-TMA	
	D_e	r_e	D_e	r_e
Reference	49.68	3.17	28.79	3.01
BLYP	—[a]	—[a]	85.74(93.59)	3.86(3.41)
BP86	—[a]	—[a]	88.95(97.00)	3.65(3.36)
PBE	—[a]	—[a]	91.74(96.61)	3.59(3.42)
B97M-V	—[a]	—[a]	69.81	3.40
BHLYP	18.12(24.27)	3.92(3.61)	32.67(40.15)	3.23(3.14)
B3LYP	-20.90(5.66)	(4.33)	53.61(61.74)	3.49(3.28)
PBE0	-11.59(8.89)	(4.11)	55.5(61.2)	3.33(3.23)
CAM-B3LYP	27.04(33.39)	3.74(3.57)	39.14(45.3)	3.18(3.13)
LC-BLYP	53.56	3.34	40.51	3.02
LC-PBE	54.16	3.25	31.28	2.93
ωB97X	54.85	3.34	36.34	3.09
ωB97X-D3(BJ)	49.39(57.64)	3.50(3.32)	29.21(37.61)	3.11(3.03)
ωB97X-V	56.79	3.36	37.31	3.05
ωB97M-V	57.21	3.33	39.54	3.04
B2GP-PLYP	25.70(29.36)	3.54(3.45)	37.74(41.36)	3.08(3.05)
SCS-B2GP-PLYP	26.36(31.67)	3.53(3.35)	27.03(33.35)	3.11(3.03)
SOS-B2GP-PLYP	26.23(31.44)	3.53(3.36)	26.85(32.91)	3.11(3.04)
B2PLYP	18.21(22.88)	3.74(3.54)	45.30(50.12)	3.22(3.16)
SOS-B2PLYP	19.05(24.76)	3.75(3.45)	35.44(42.85)	3.24(3.09)
PBE-QIDH	29.80(32.08)	3.45(3.42)	37.85(39.74)	3.01(3.00)
SCS-PBE-QIDH	30.07(32.63)	3.40(3.37)	31.44(33.68)	3.01(3.00)
SOS-PBE-QIDH	30.29(33.28)	3.39(3.35)	28.73(31.36)	3.02(3.01)
PBE0-DH	18.44(22.69)	3.75(3.59)	45.11(49.83)	3.15(3.10)
RSX-0DH	53.10(54.49)	3.24(3.24)	31.34(32.28)	2.93(2.93)
RSX-QIDH	51.59(51.89)	3.23(3.23)	31.18(31.44)	2.90(2.90)
SCS-RSX-QIDH	49.17(49.19)	3.23(3.23)	34.97(34.99)	2.87(2.87)
SOS-RSX-QIDH	51.80(52.12)	3.17(3.17)	22.67(22.97)	2.89(2.89)
ωB2GP-PLYP	51.13(51.14)	3.27(3.27)	30.72(30.72)	2.94(2.94)
SCS-ωB2GP-PLYP	50.42(51.43)	3.27(3.26)	23.72(24.64)	2.95(2.95)
SOS-ωB2GP-PLYP	51.24(52.26)	3.25(3.25)	21.40(22.33)	2.95(2.95)
ωB2PLYP	51.80(51.96)	3.28(3.28)	32.74(32.89)	2.97(2.97)
SOS-ωB2PLYP	51.90(53.32)	3.27(3.26)	25.68(26.74)	2.98(2.97)
ωB88PP86	50.88(50.88)	3.23(3.23)	42.21(42.21)	2.91(2.91)
SCS-ωB88PP86	50.38(50.46)	3.24(3.24)	31.63(31.71)	2.94(2.94)
SOS-ωB88PP86	50.87(50.94)	3.23(3.23)	29.67(29.74)	2.95(2.95)
ωPBEPP86	52.23(52.23)	3.17(3.17)	44.80(44.80)	2.87(2.87)
SCS-ωPBEPP86	50.02(50.03)	3.22(3.22)	35.60(35.61)	2.91(2.91)
SOS-ωPBEPP86	52.02(52.02)	3.18(3.18)	30.01(30.01)	2.91(2.91)

[a] Did not give the correct dissociation curves, see main aticle.

3 Dissociation curves

3.1 Spin-scaled double-hybrid DFAs

Dissociation curves are shown for all exicplexes for TD-SCS/SOS-DHDFAs, with and without the D3(BJ) dispersion correction. For ease of viewing, these are shown with global methods on the left and RS methods in the centre and right panels. For some TD-(SCS/SOS)-DHDFAs, the SCS and SOS variants produce overlapping dissociation curves. Additionally, for some RS TD-(SCS/SOS)-DHDFAs the D3(BJ) correction has no impact on the dissociation curve.

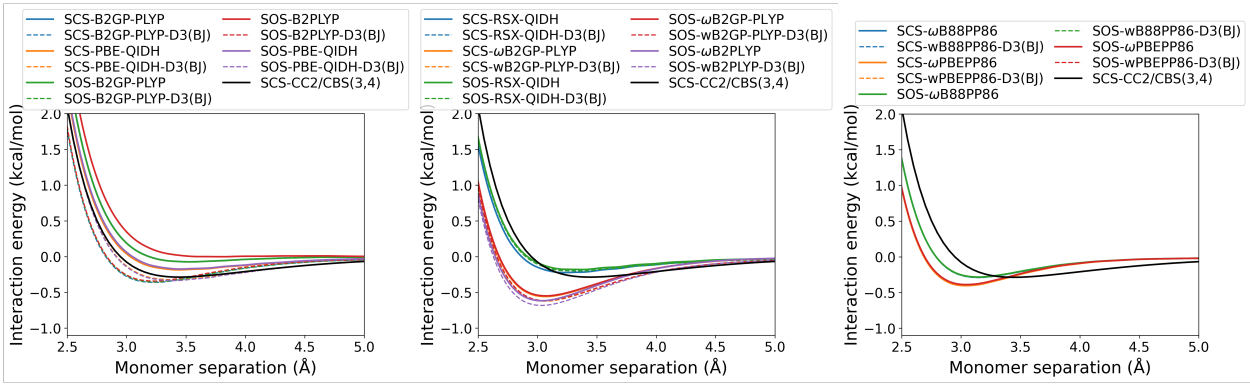

Figure S2: Benzene-neon dissociation curves for TD-SCS/SOS-DHDFAs calculated for the lowest-lying singlet excited state. The D3(BJ) dispersion correction results in overlapping dissociation curves for some RS TD-(SCS/SOS)-DHDFAs.

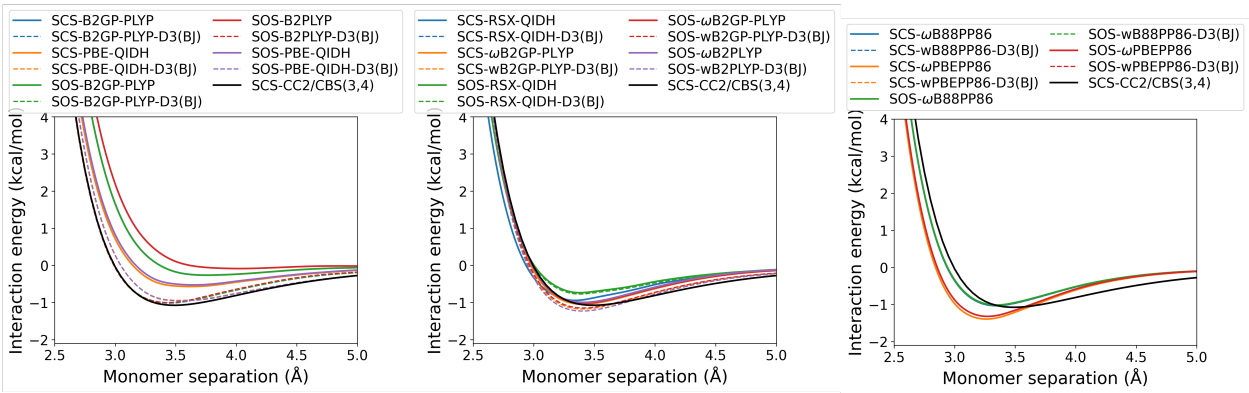

Figure S3: Benzene-argon dissociation curves for TD-SCS/SOS-DHDFAs calculated for the lowest-lying singlet excited state. The D3(BJ) dispersion correction results in overlapping dissociation curves for some RS TD-(SCS/SOS)-DHDFAs.

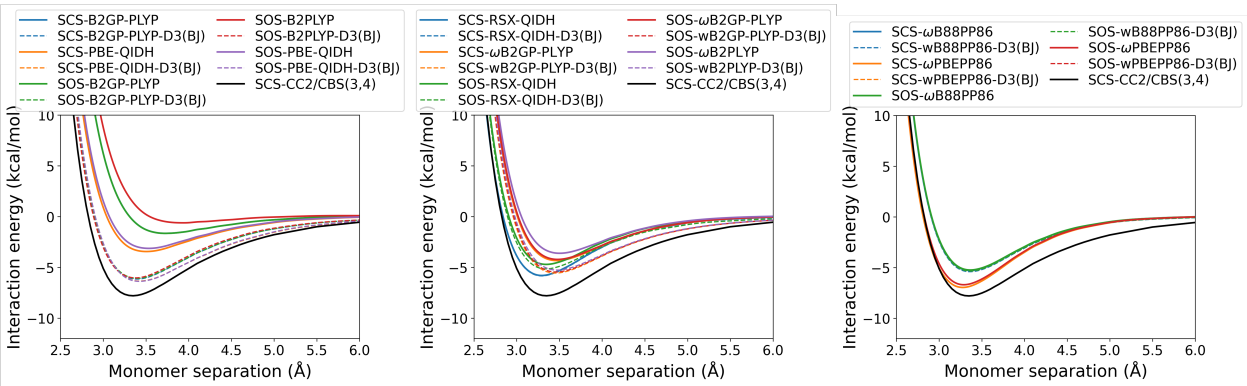

Figure S4: Benzene-anthracene dissociation curves for TD-SCS/SOS-DHDFAs calculated for the lowest-lying singlet excited state. The D3(BJ) dispersion correction results in overlapping dissociation curves for some RS TD-(SCS/SOS)-DHDFAs.

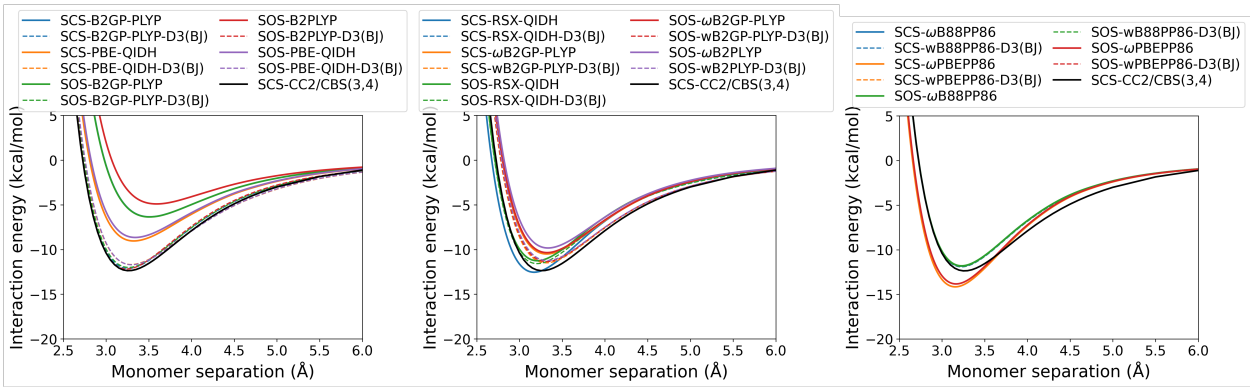

Figure S5: Toluene-TCNE dissociation curves for TD-SCS/SOS-DHDFAs calculated for the 3A' state. The D3(BJ) dispersion correction results in overlapping dissociation curves for some RS TD-(SCS/SOS)-DHDFAs.

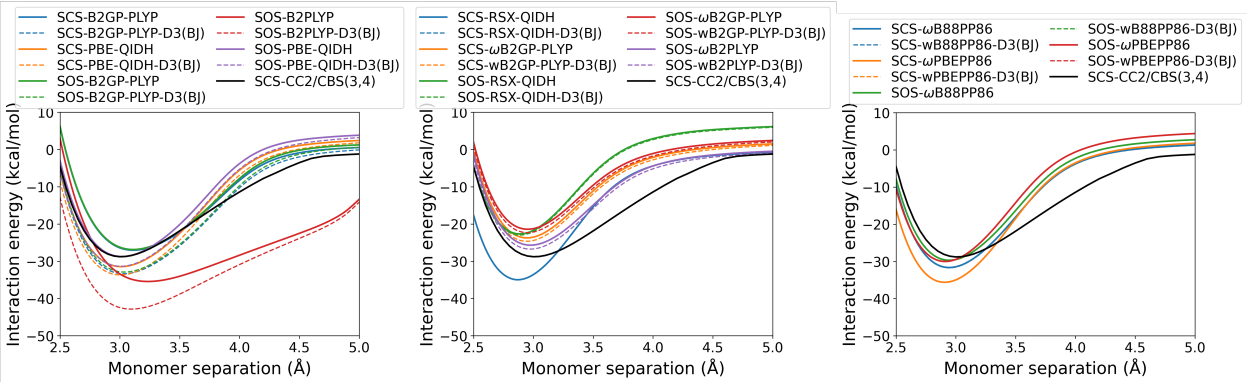

Figure S6: Styrene-TMA dissociation curves for TD-SCS/SOS-DHDFAs calculated for the lowest-lying singlet excited state. The D3(BJ) dispersion correction results in overlapping dissociation curves for some RS TD-(SCS/SOS)-DHDFAs.

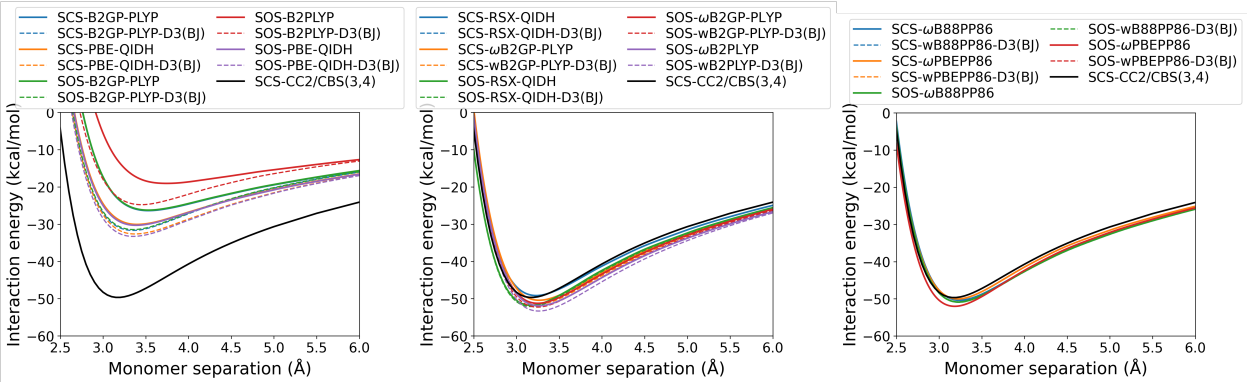

Figure S7: Toluene-TCNE dissociation curves for TD-SCS/SOS-DHDFAs calculated for the 2A' state. The D3(BJ) dispersion correction results in overlapping dissociation curves for some RS TD-(SCS/SOS)-DHDFAs.

3.2 DFT-D3(BJ) dispersion-corrected DFAs

In this section, dissociation curves are shown which include the DFT-D3(BJ) dispersion correction. The D3(BJ)-corrected global hybrid DFAs are given in the main body and the D3(BJ)-corrected TD-SCS/SOS-DHDFAs are in Section 3.1. Dissociation curves are presented by GGA (top left), RS hybrid (top right), global double hybrid (bottom left) and RS double hybrid (bottom right). For some RS TD-DHDFAs, D3(BJ) has no impact on the dissociation curves. We also provide dissociation curves for benzene-argon with the re-fitted D3(BJ) corrections for ωB2GP-PLYP, ωB2PLYP, and RSX-QIDH.[S6] This re-fit has no impact on the dissociation curves, see Figure S14.

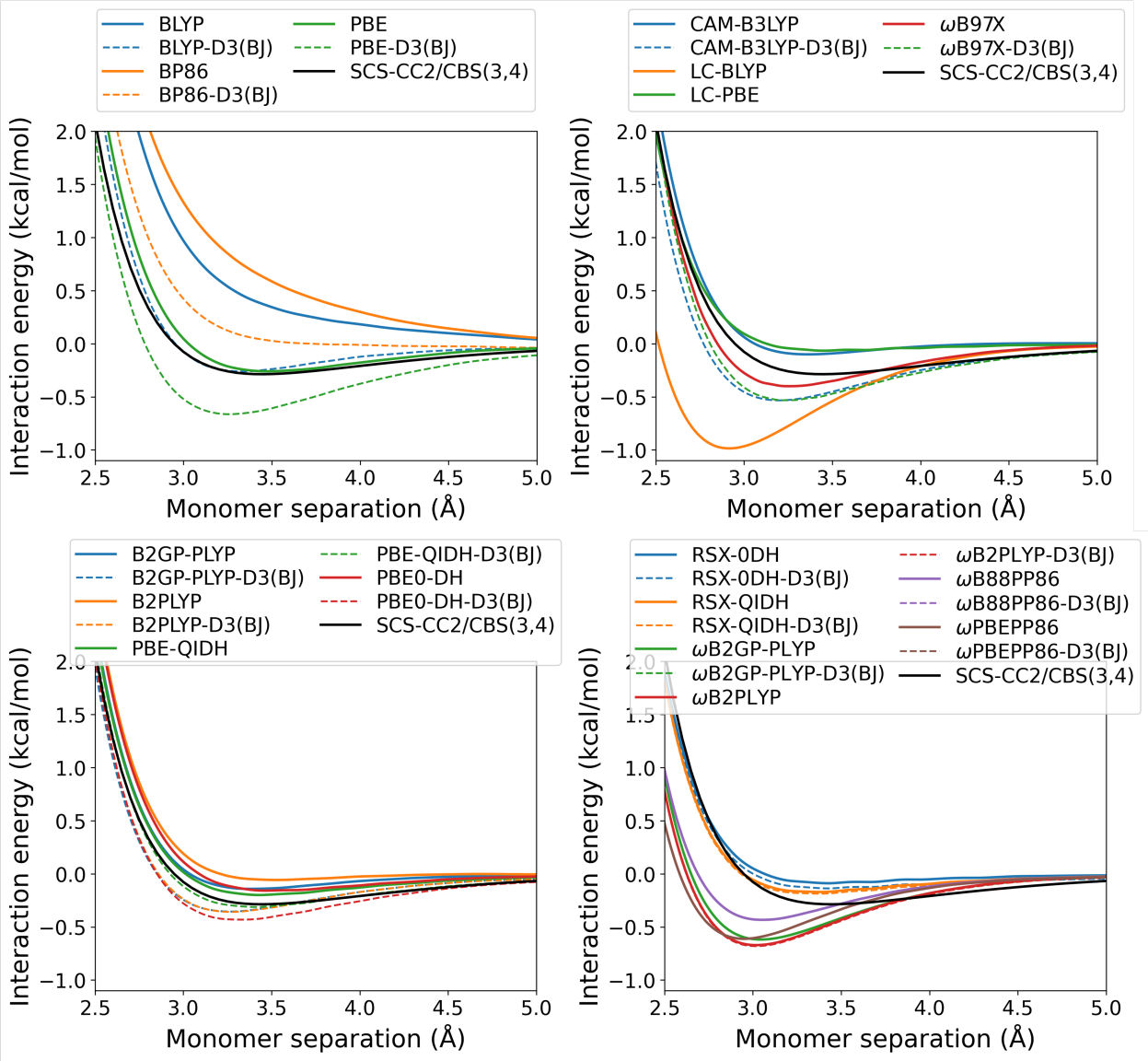

Figure S8: Benzene-neon dissociation curves calculated for the lowest-lying singlet excited state shown with and without the D3(BJ) dispersion correction. The D3(BJ) dispersion correction results in overlapping dissociation curves for some RS TD-DHDFAs.

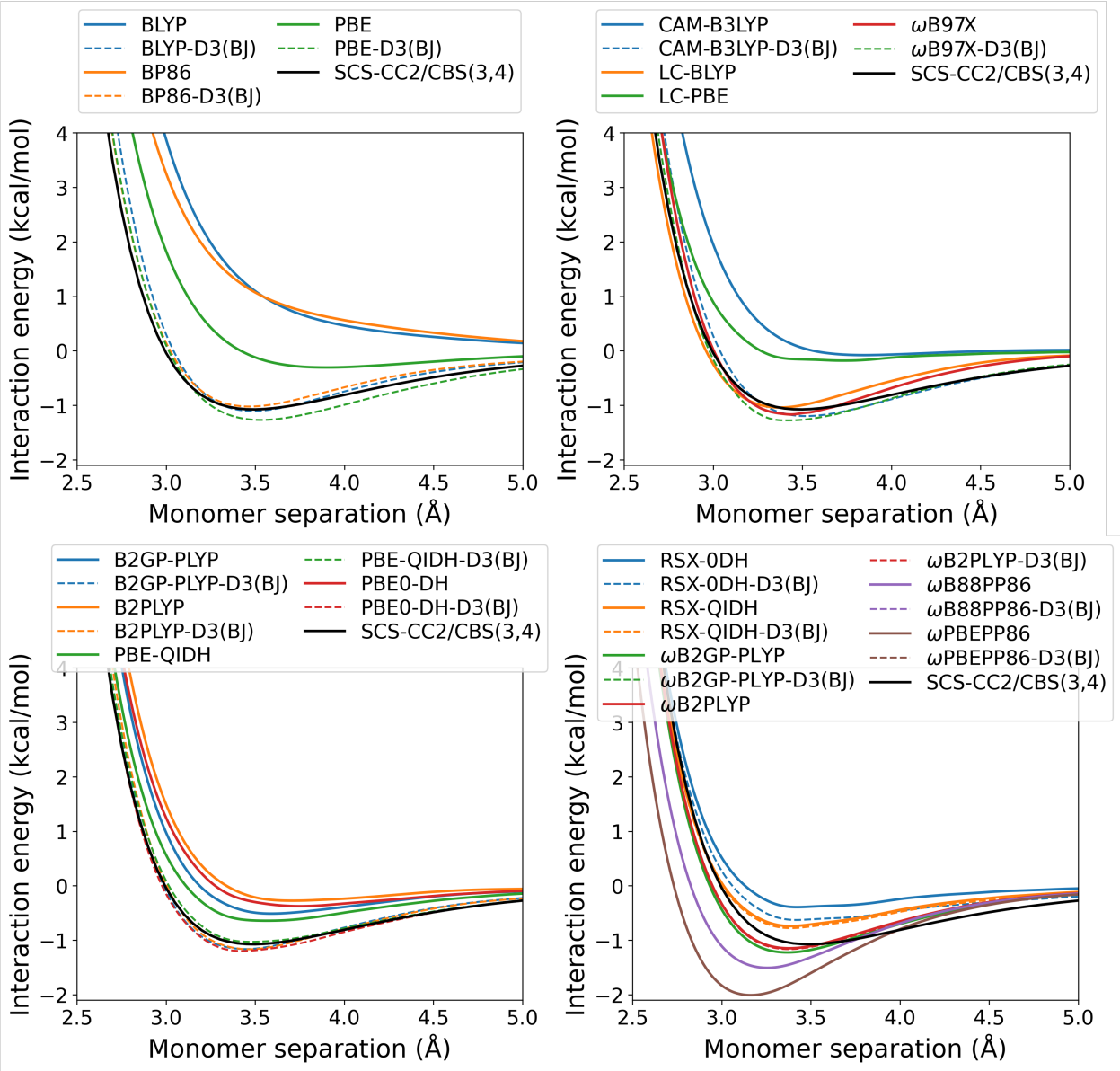

Figure S9: Benzene-argon dissociation curves calculated for the lowest-lying singlet excited state shown with and without the D3(BJ) dispersion correction. The D3(BJ) dispersion correction results in overlapping dissociation curves for some RS TD-DHDFAs.

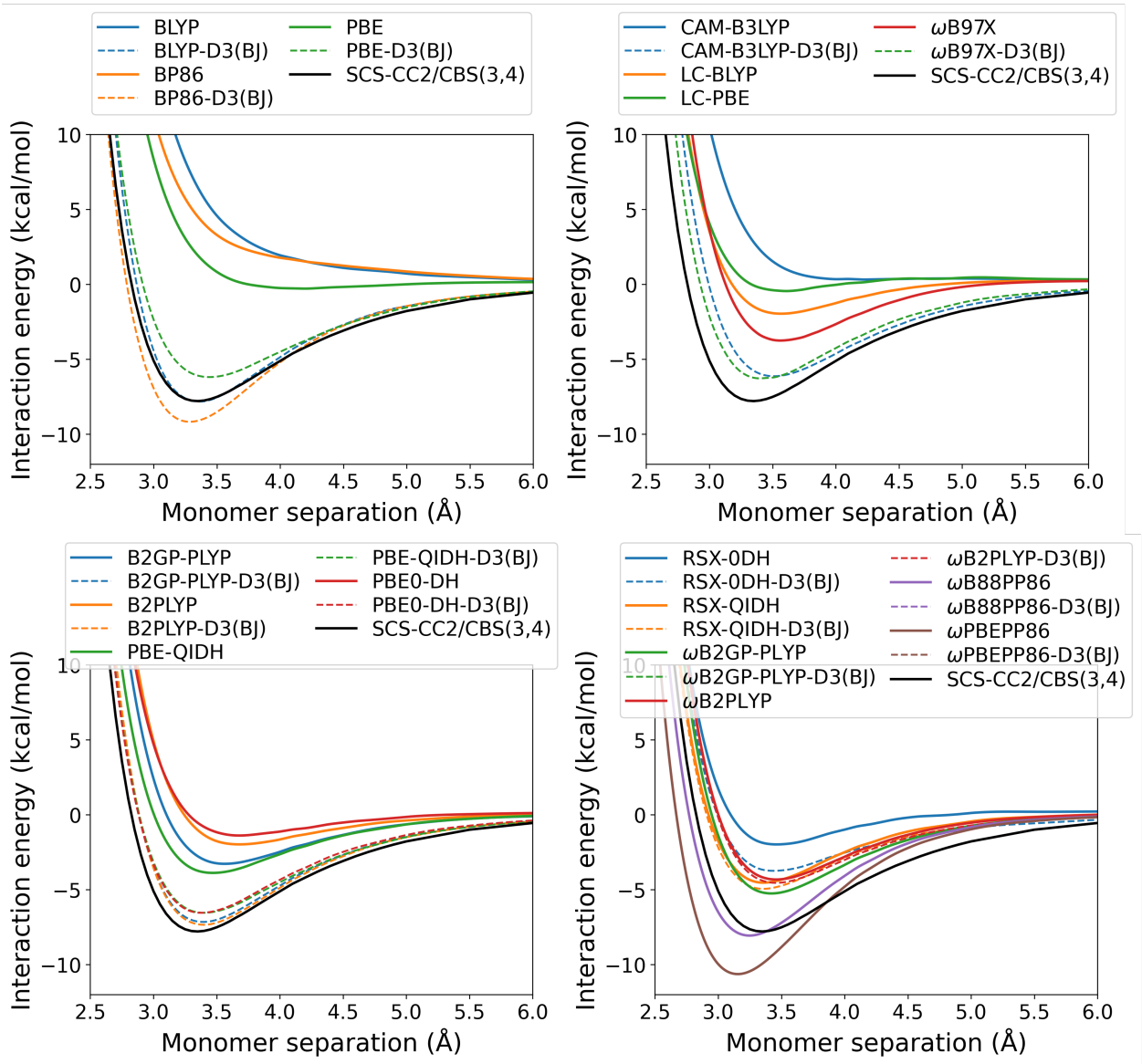

Figure S10: Benzene-anthracene dissociation curves calculated for the lowest-lying singlet excited state shown with and without the D3(BJ) dispersion correction. The D3(BJ) dispersion correction results in overlapping dissociation curves for some RS TD-DHDFAs.

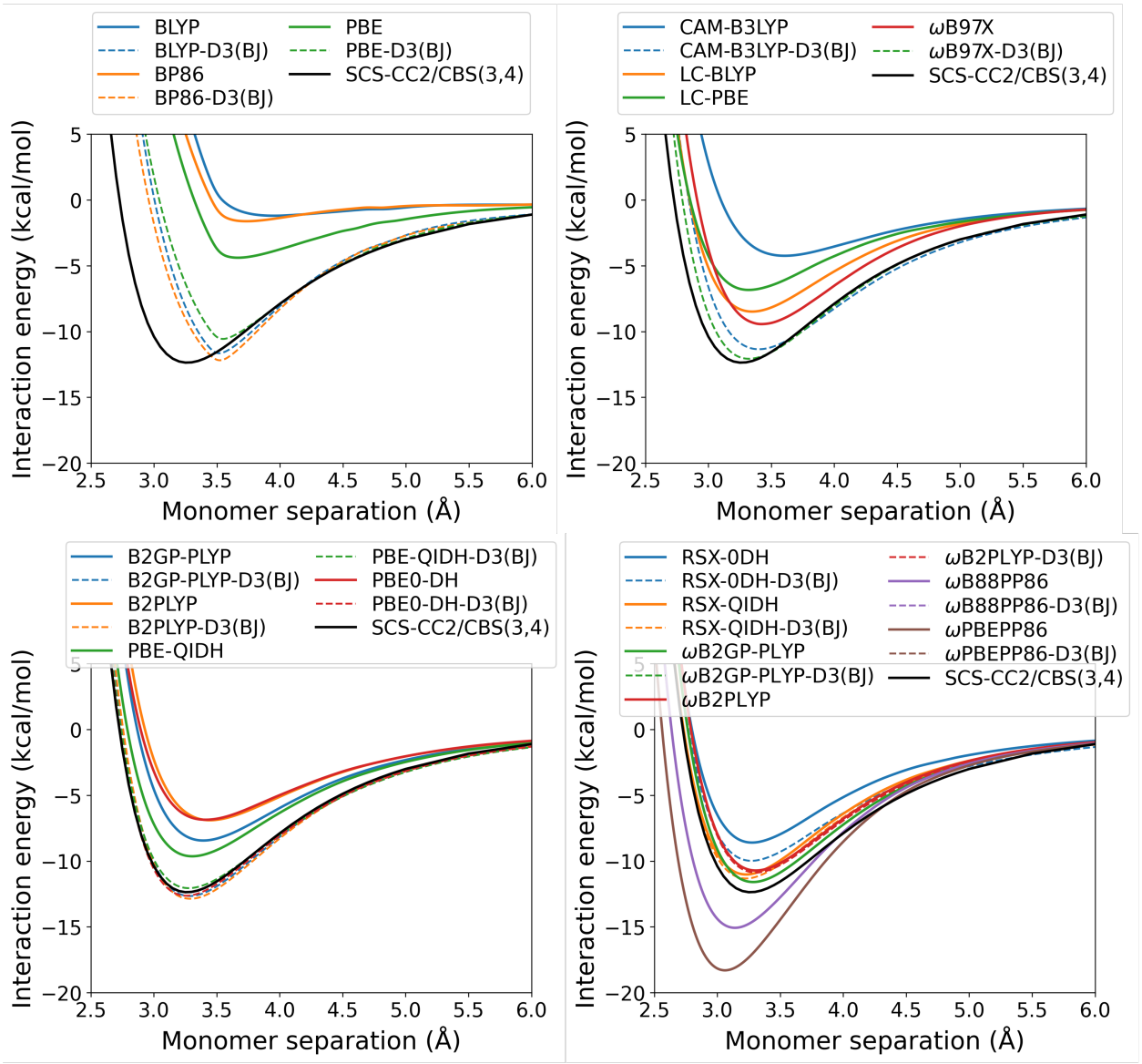

Figure S11: Toluene-TCNE dissociation curves calculated for the 3A' state shown with and without the D3(BJ) dispersion correction. The D3(BJ) dispersion correction results in overlapping dissociation curves for some RS TD-DHDFAs.

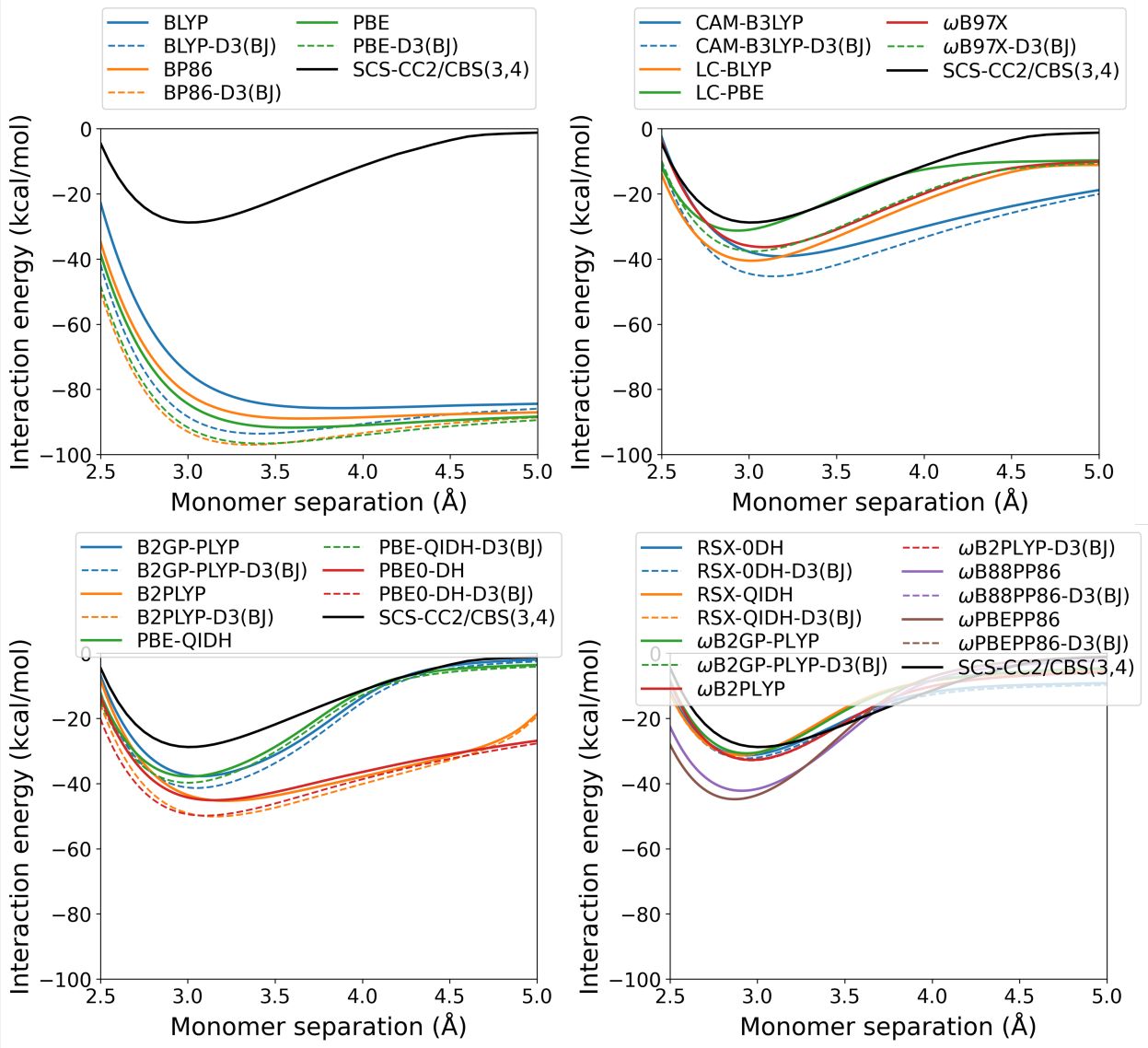

Figure S12: Styrene-TMA dissociation curves calculated for the lowest-lying singlet excited state shown with and without the D3(BJ) dispersion correction. The D3(BJ) dispersion correction results in overlapping dissociation curves for some RS TD-DHDFAs.

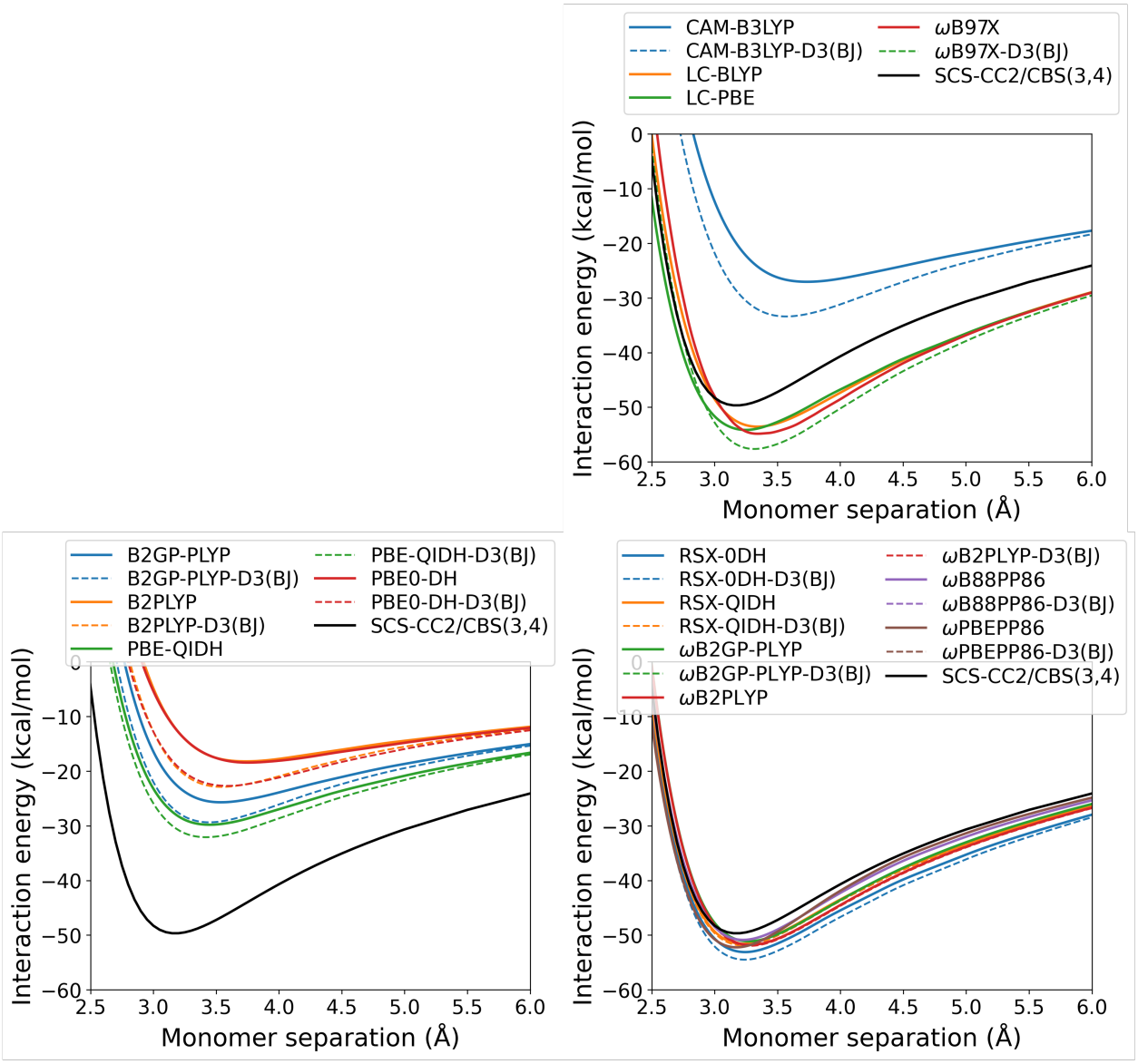

Figure S13: Toluene-TCNE dissociation curves calculated for the 2A' excited state shown with and without the D3(BJ) dispersion correction. The D3(BJ) dispersion correction results in overlapping dissociation curves for some RS TD-DHDFAs. Dissociation curves could not be obtained for this state with the GGA methods as discussed in the main text.

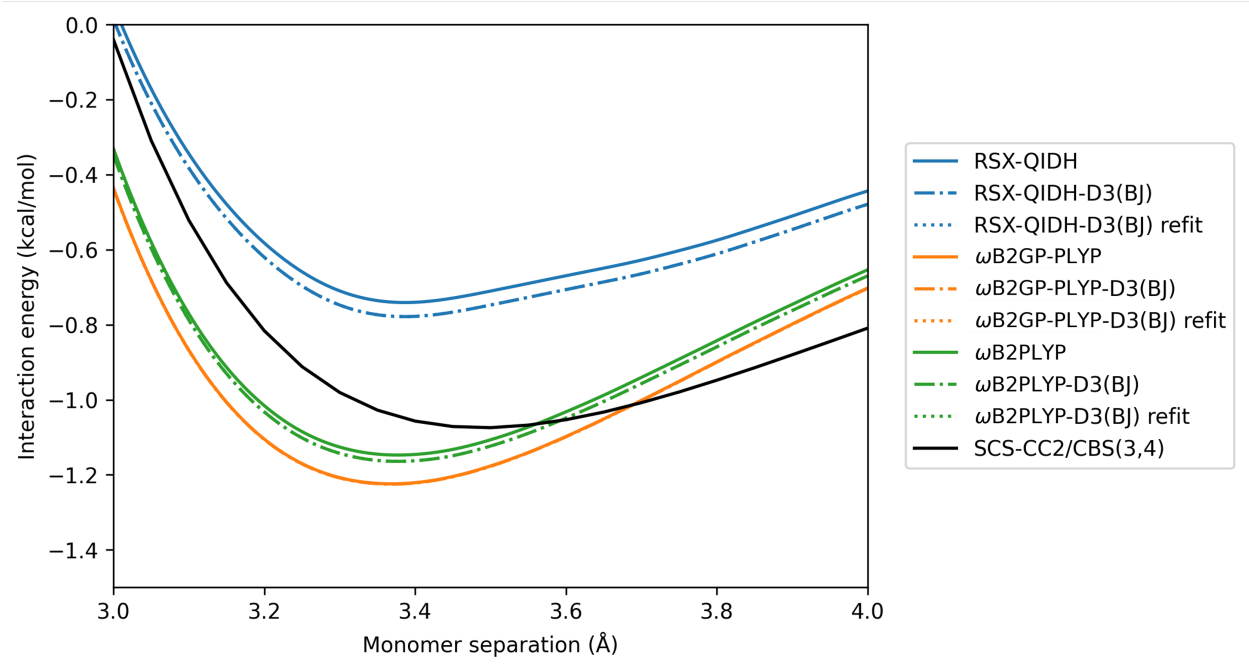

Figure S14: Benzene-argon exciplex dissociation curves for RS TD-DHDFAs with the refitted D3(BJ) dispersion correction. The refitted D3(BJ) correction makes no difference to the dissociation curve compared to the original parameterisation. Additionally, for ωB2GP-PLYP the dispersion-corrected dissociation curves overlap with that of the dispersion-uncorrected method.

4 Exciplexes with CT transitions

4.1 Orbital pictures

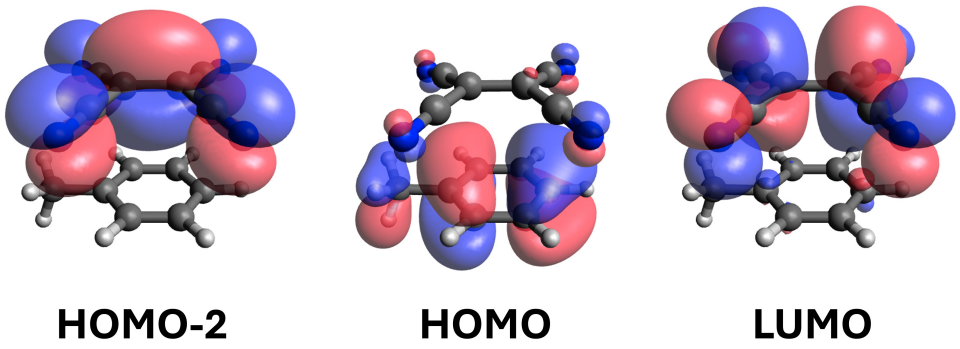

Figure S15: Relevant molecular orbitals for the toluene-TCNE dimer calculated at the HF/def2-QZVP level of theory. The 2A' excitation is a HOMO to LUMO transition and the 3A' excitation is a HOMO-2 to LUMO one.

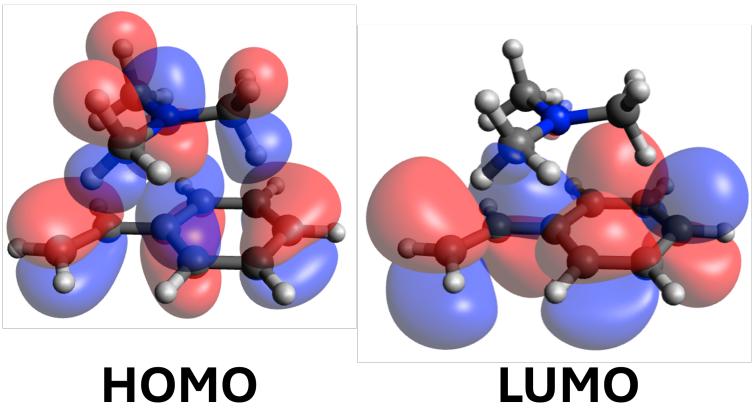

Figure S16: Relevant molecular orbitals for the styrene-TMA dimer calculated at the HF/def2-QZVP level of theory.

4.2 Styrene-TMA excitation energies

Table S3: Excitation energies in eV for the styrene-TMA exciplex calculated near the equilibrium geometry (3 Å) and at the 16 Å endpoint. SCS-CC2/def2-QZVP is shown for reference. Note that the D3(BJ) dispersion correction has no bearing on the calculated excitation energy.

	Excitation energy (eV)	
Method	3 Å	16 Å
SCS-CC2/def2-QZVP	3.11	4.63
BLYP	1.08	5.17
BP86	1.01	5.21
PBE	0.98	5.21
B97M-V	1.51	4.62
BHLYP	3.04	5.05
B3LYP	1.85	4.67
PBE0	1.96	4.78
CAM-B3LYP	2.70	4.94
LC-BLYP	2.91	4.98
LC-PBE	3.49	5.19
ωB97X	3.13	5.06
ωB97X-D3(BJ)	3.18	5.06
ωB97X-V	3.15	5.07
ωB97M-V	3.04	5.01
B2GP-PLYP	2.63	4.68
SCS-B2GP-PLYP	2.97	4.65
SOS-B2GP-PLYP	2.92	4.59
B2PLYP	2.24	4.63
SOS-B2PLYP	2.81	4.87
PBE-QIDH	2.84	4.81
SCS-PBE-QIDH	2.80	4.52
SOS-PBE-QIDH	2.83	4.45
PBE-0DH	2.51	4.87
RSX-0DH	3.48	5.13
RSX-QIDH	3.41	4.97
SCS-RSX-QIDH	3.00	4.65
SOS-RSX-QIDH	3.12	4.29
ωB2GP-PLYP	3.31	4.87
SCS-ωB2GP-PLYP	3.20	4.52
SOS-ωB2GP-PLYP	3.27	4.49
ωB2PLYP	3.23	4.91
SOS-ωB2PLYP	3.21	4.63
ωB88PP86	2.89	4.78
SCS-ωB88PP86	3.00	4.58
SOS-ωB88PP86	2.99	4.48
ωPBEPP86	2.90	4.75
SCS-ωPBEPP86	2.86	4.51
SOS-ωPBEPP86	2.98	4.38

5 ALMO-EDA

In the ALMO-EDA scheme by Ge et al., the Pauli repulsion term is known to suffer from contamination by dispersion. We verified this by performing ALMO-EDA calculations with a dispersion-uncorrected DFA. For technical reasons, it was not possible to perform ALMO-EDA calculations with ωB97M in QCHEM. Instead, we tested CAM-B3LYP which is also a dispersion-uncorrected RS hybrid. The results for the benzene-argon exciplex are shown as a case study in Figure S17, for both dispersion-uncorrected CAM-B3LYP and CAM-B3LYP-D3(BJ). From this case study, the only effect of the D3(BJ) correction is to the Pauli term in the ALMO-EDA calculation. This becomes uphysically attractive when the D3(BJ) correction is added, which indeed shows that this term is contaminated by dispersion in the ALMO-EDA scheme. Additionally, the D3(BJ) correction gives rise to an overall stabilisation of 1.25 kcal mol^{-1} to the overall ALMO-EDA. This supports that dispersion is the dominant contribution to the binding strength for the benzene-argon exciplex.

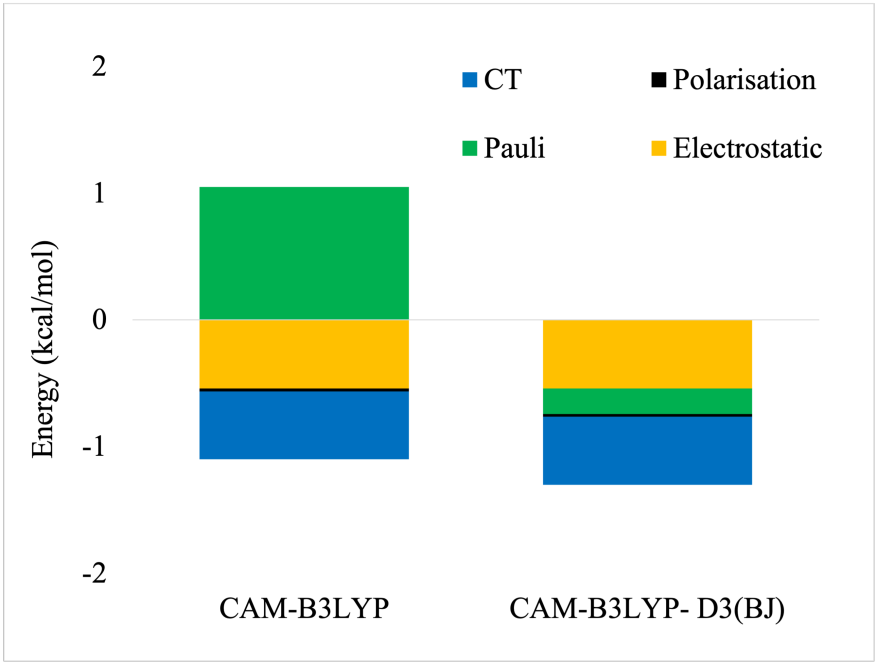

Figure S17: Stacked energy diagram for ALMO-EDA of benzene-argon exciplex, calculated with CAM-B3LYP with and without the D3(BJ) correction and with the def2-TZVP basis set.

6 CT statistics

In this section, we present CT metrics developed by Plasser and Lischka, which use the one-electron transition density matrix.[S7] The CT number varies from 0 for localised excitations to 1 for charge-separated excitations. A participation ratio (PR) measures the delocalisation of the excitation over fragments, with PR=1 for localised excitations and PR=2 when the excitation is equally shared between fragments. Finally, the average excitation position (POS) can be calculated and POS=1.5 indicates an entirely delocalised excitation whereas POS=1 or POS=2 indicate localisation on fragments 1 or 2 respectively. The calculated CT metrics are shown in Table S4.

The TD-DFT methods tested generally have excellent agreement with the SCS-CC2 reference. However, for styrene-TMA these methods show highly variable performance. This can be rationalised in terms of the MOs involved for the calculated excitation. The lowest singlet excitation for styrene-TMA is predominantly a HOMO-LUMO transition but also involves a significant contribution from HOMO-1 to LUMO (18% contribution for the reference method). HOMO-1 involves both monomers but has larger lobes on styrene. Hence, the (HOMO-1)-LUMO transition has less CT character compared to the HOMO-LUMO one.

However, not all TD-DFT methods correctly predict this contribution from HOMO-1. For example, PBE predicts that the lowest singlet excitation is purely a HOMO-LUMO transition. As such, PBE overestimates the CT number for styrene-TMA. On the other hand, ωB88PP86 predicts a dominant HOMO-LUMO transition but also contribution from HOMO-1 to LUMO which is qualitatively correct for the lowest singlet excitation. Correspondingly, the calculated CT number is small for ωB88PP86. For styrene-TMA, we calculated CT numbers for 20 TD-DFT methods and verify a strong correlation between the CT number and the proportion of the excitation which is a HOMO-LUMO transition.

Table S4: CT metrics for exciplexes in their equilibrium geometry, optimised with SCS-CC2/def2-TZVP. CT metrics were calculated using the one-electron transition density matrix obtained from various methods with the def2-QZVP basis set. The designated fragment number is shown in brackets

Exciplex	Method	CT	PR	POS
Benzene(1)-neon(2)	SCS-CC2	0.00	1.00	1.00
	PBE	0.00	1.00	1.00
	LC-BLYP	0.00	1.00	1.00
	ωB88PP86	0.00	1.00	1.00
Benzene(1)-argon(2)	SCS-CC2	0.00	1.00	1.00
	PBE	0.00	1.00	1.00
	LC-BLYP	0.00	1.00	1.00
	ωB88PP86	0.00	1.00	1.00
Benzene(1)-anthracene(2)	SCS-CC2	0.04	1.05	1.98
	PBE	0.10	1.11	1.95
	LC-BLYP	0.04	1.05	1.98
	ωB88PP86	0.04	1.05	1.98
Toluene(1)-TCNE(2) 3A'	SCS-CC2	0.04	1.07	1.97
	PBE[a]	0.09	1.11	1.95
	LC-BLYP	0.04	1.06	1.97
	ωB88PP86	0.04	1.06	1.97
Toluene(1)-TCNE(2) 2A'	SCS-CC2	0.92	1.09	1.51
	PBE[a]	0.93	1.08	1.50
	LC-BLYP	0.92	1.09	1.51
	ωB88PP86	0.91	1.10	1.51
Styrene(1)-TMA(2)	SCS-CC2	0.83	1.20	1.47
	PBE	0.93	1.08	1.50
	LC-BLYP	0.81	1.22	1.46
	ωB88PP86	0.55	1.54	1.32

[a]PBE calculations use the 3.7 Å exciplex geometry for toluene-TCNE

CT refers to Charge Transfer number, PR is Participation Ratio and POS is average excitation position

7 MAEs

7.1 Overall MAEs

The overall MAEs are shown for all exciplexes, both localised and CT, in Figure S18 for D_e and Figure S19 for r_e.

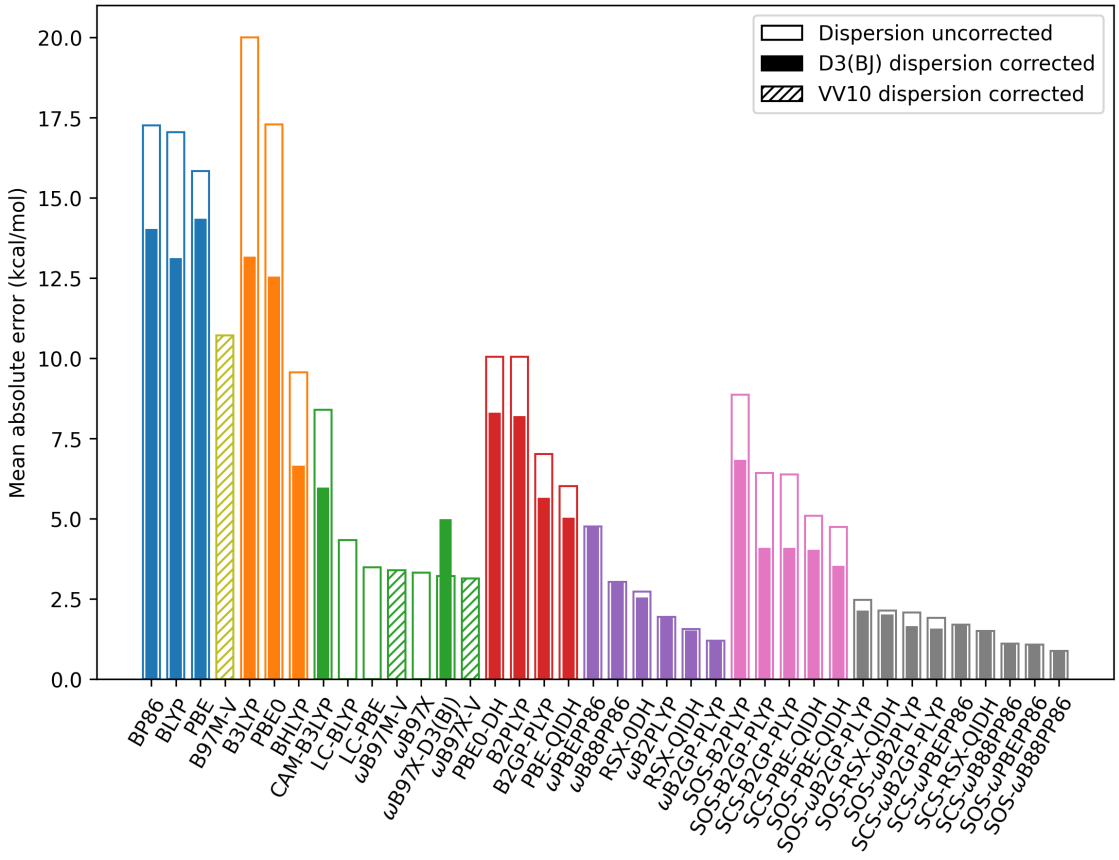

Figure S18: MAEs for all exciplexes for D_e in kcal mol^{-1}.

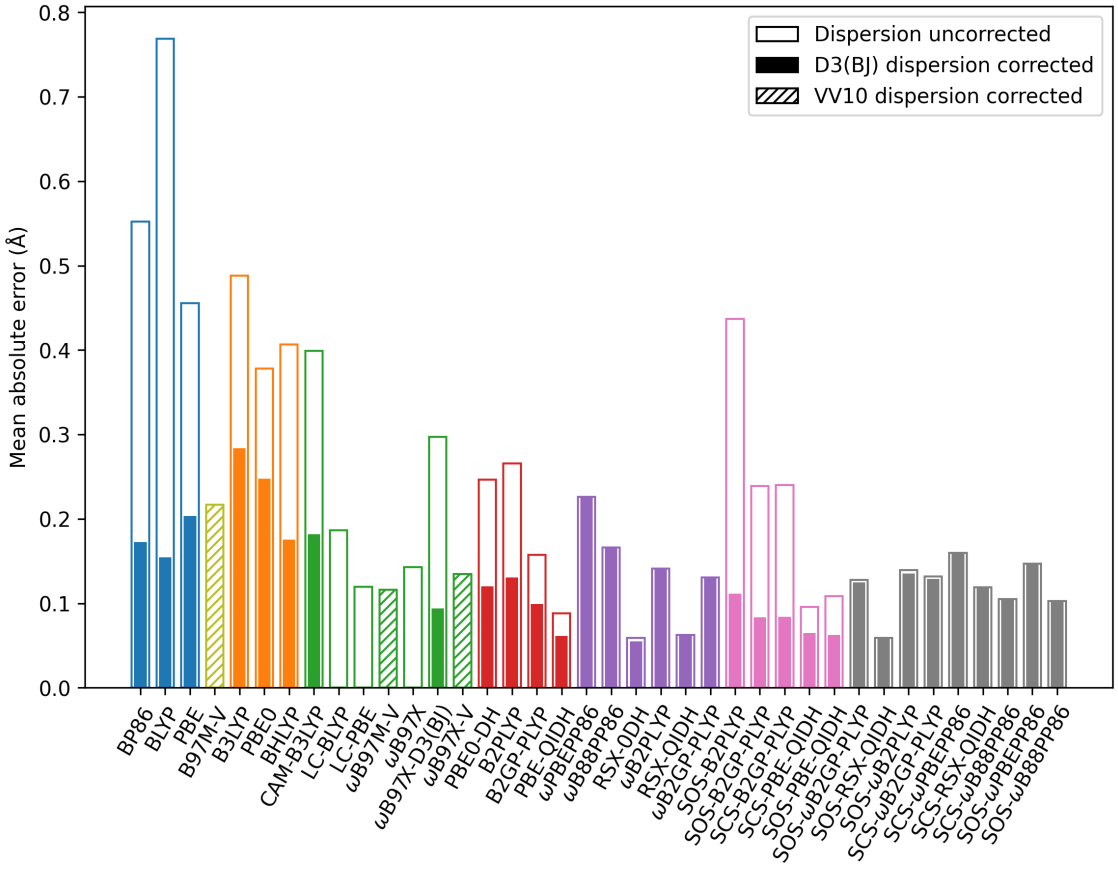

Figure S19: MAEs for all exciplexes for r_e in Å.

7.2 Exciplexes with localised excitations

The MAEs for r_e in Å are given for exciplexes with a localised excitation (benzene-neon, benzene-argon, benzene-anthracene, and toluene-TCNE 3A'.) in Figure S20. MAEs for D_e in kcal mol^{-1} are presented in the main body.

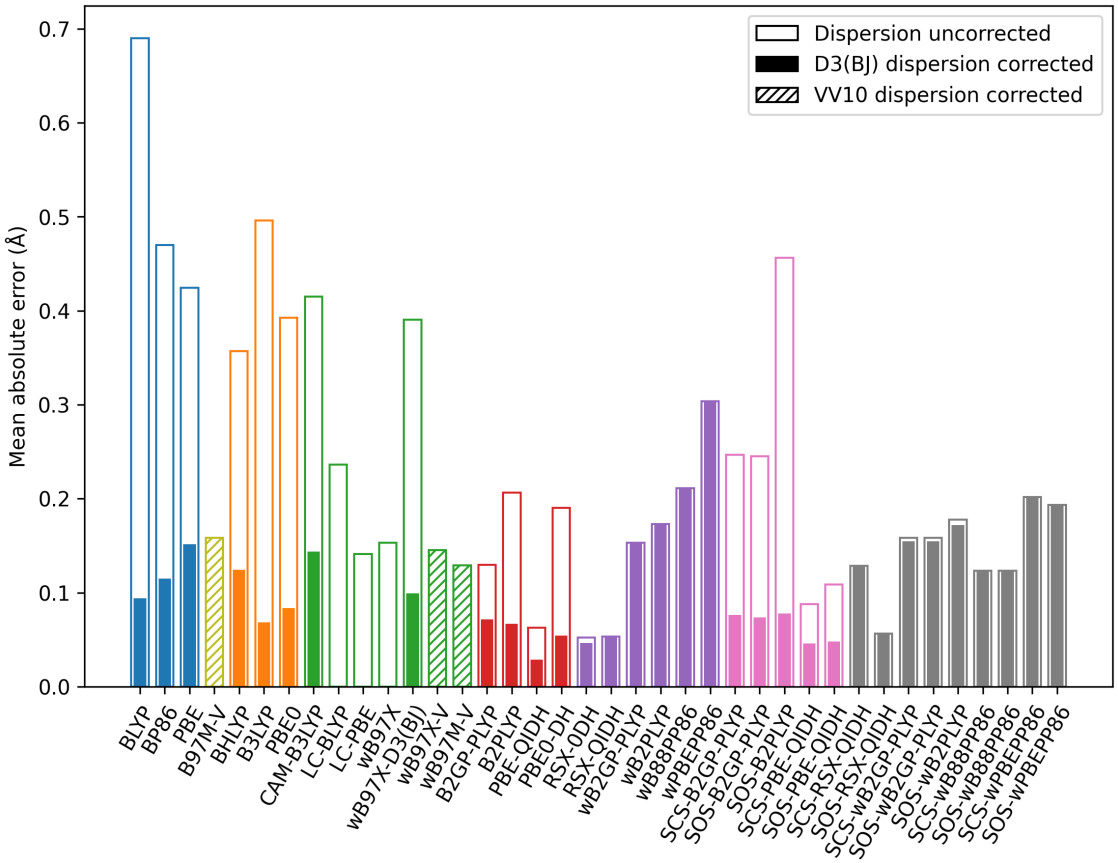

Figure S20: MAEs for exciplexes with a localised excitation for r_e in Å.

7.3 Non-equilibrium geometry

For the exciplexes with a localised excitation, MAEs were also calculated for non-equilibrium geometries in the spirit of the S66X8 dataset as detailed in the main article. MAEs were calculated at 8 geometries per system by scaling the respective equilibrium distance by 0.90, 0.95, 1.00, 1.05, 1.10, 1.25, 1.50 and 2.00. These MAEs are averaged and shown in in Figure S21 for D_e. The MAPEs are for D_e are given in Figure S22, expressed in %.

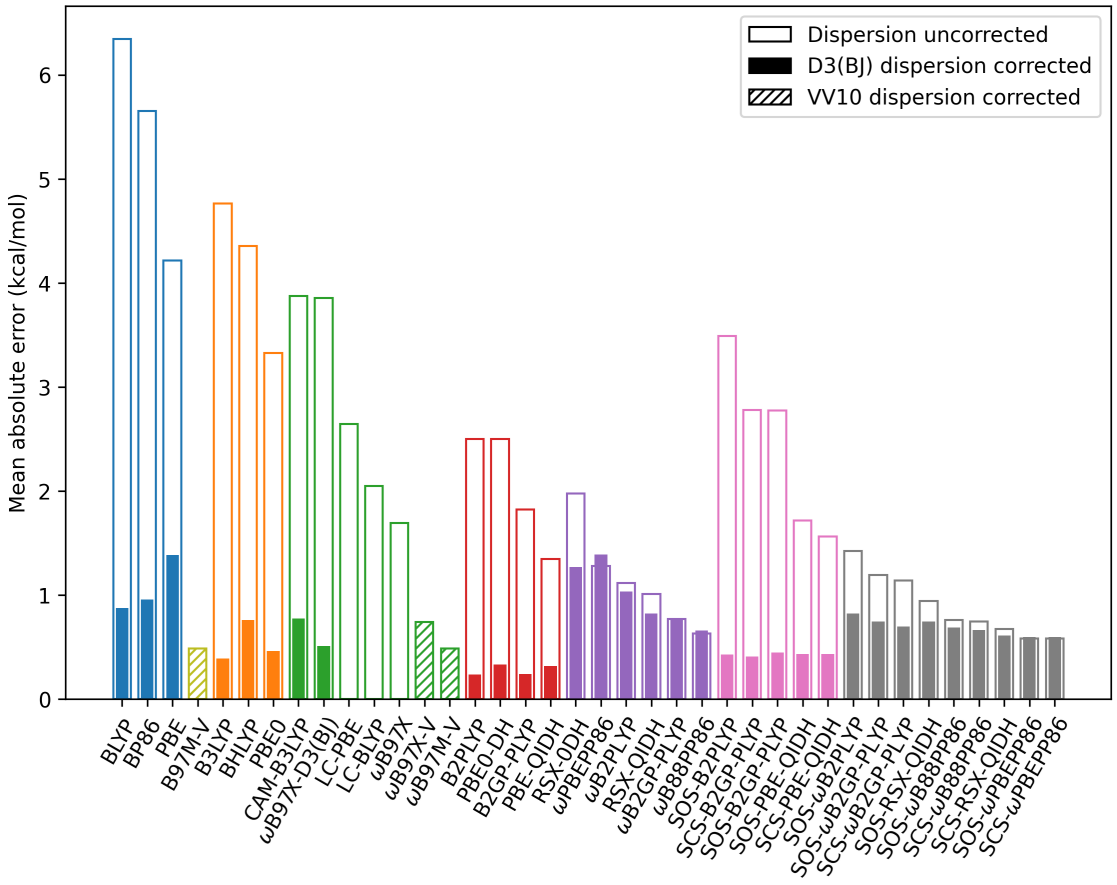

Figure S21: MAEs for exciplexes with a localised excitation for D_e in kcal mol^{-1}, averaged over 8 geometries per system along the dissociation curve.

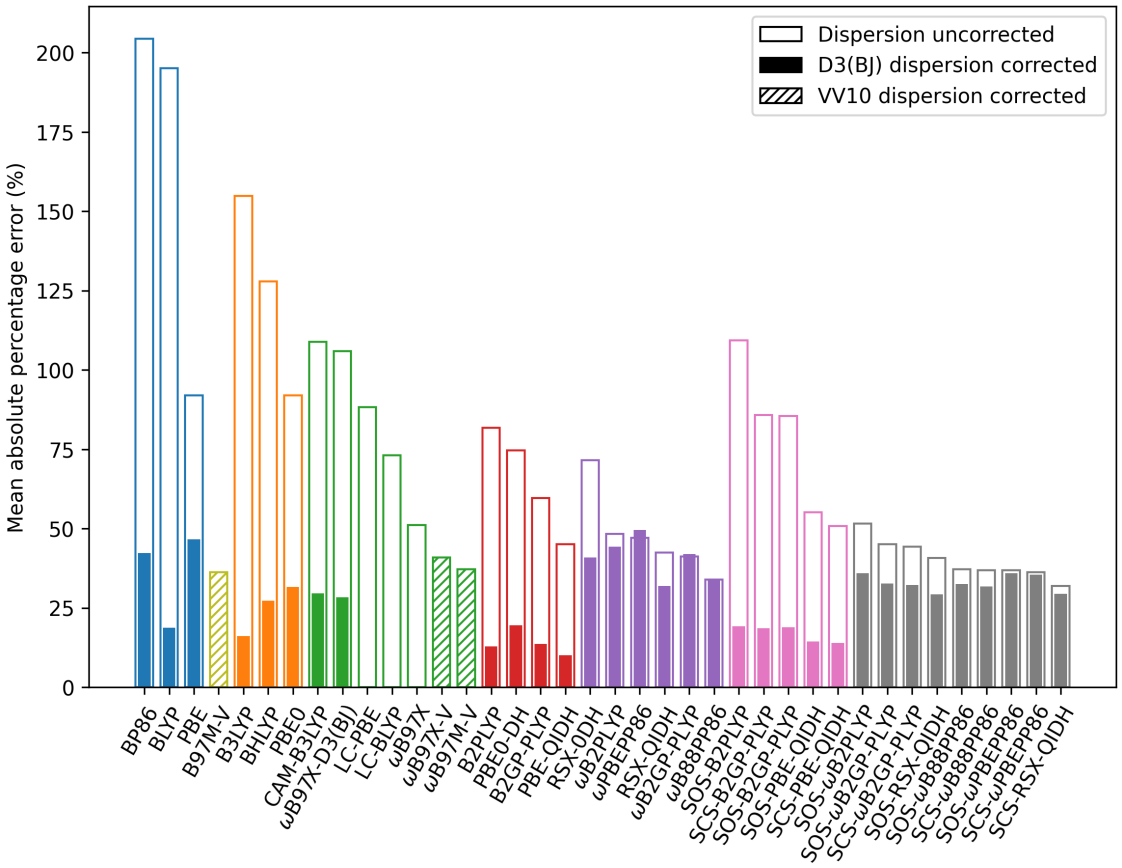

Figure S22: MAPEs for exciplexes with a localised excitation for D_e in %, averaged over 8 geometries per system along the dissociation curve.

7.4 Tabulated MAE data

Table S5: Values for MAE are given in terms of dissociation energies (D_e, kcal mol^{-1}) and equilibrium distances (r_e, Å) for TD-DFT methods. MAEs are presented separately for exciplexes with a localised excitation and for all exciplexes. Where the D3(BJ) correction is available for a method, the dispersion-corrected value is shown in parentheses.

Method	Localised		All exciplexes	
	D_e	r_e	D_e	r_e
BLYP	7.08(0.20)	0.69(0.09)	17.06(13.12)	0.77(0.15)
BP86	6.54(0.49)	0.47(0.12)	17.27(14.03)	0.55(0.17)
PBE	4.07(0.99)	0.42(0.15)	15.84(14.36)	0.46(0.20)
B97M-V	0.61	0.16	10.71	0.22
BHLYP	5.48(0.79)	0.36(0.12)	9.56(6.65)	0.41(0.18)
B3LYP	6.15(0.51)	0.50(0.07)	20.00(13.17)	0.49(0.28)
PBE0	3.95(0.52)	0.39(0.08)	17.30(12.55)	0.38(0.25)
CAM-B3LYP	4.35(0.76)	0.42(0.14)	8.40(5.97)	0.40(0.18)
LC-BLYP	2.61	0.24	4.34	0.19
LC-PBE	3.5	0.14	3.49	0.12
ωB97X	1.79	0.15	3.32	0.14
ωB97X-D3(BJ)	4.15(0.57)	0.39(0.10)	3.22(4.99)	0.30(0.09)
ωB97X-V	0.79	0.15	3.13	0.13
ωB97M-V	0.52	0.13	3.39	0.12
B2GP-PLYP	2.29(0.27)	0.13(0.07)	7.01(5.66)	0.16(0.10)
SCS-B2GP-PLYP	3.30(0.51)	0.25(0.08)	6.38(4.10)	0.24(0.08)
SOS-B2GP-PLYP	3.30(0.55)	0.25(0.07)	6.43(4.09)	0.24(0.08)
B2PLYP	3.08(0.28)	0.21(0.07)	10.05(8.21)	0.27(0.13)
SOS-B2PLYP	3.98(0.52)	0.46(0.08)	8.87(6.84)	0.44(0.11)
PBE-QIDH	1.79(0.41)	0.06(0.03)	6.02(5.03)	0.09(0.06)
SCS-PBE-QIDH	2.07(0.58)	0.09(0.05)	5.09(4.04)	0.10(0.06)
SOS-PBE-QIDH	2.26(0.56)	0.11(0.05)	4.75(3.54)	0.11(0.06)
PBE0-DH	3.19(0.45)	0.19(0.05)	10.05(8.30)	0.25(0.12)
RSX-0DH	2.62(1.76)	0.05(0.05)	2.74(2.56)	0.06(0.05)
RSX-QIDH	1.26(1.07)	0.05(0.05)	1.56(1.53)	0.06(0.06)
SCS-RSX-QIDH	0.59(0.59)	0.13(0.13)	1.51(1.51)	0.12(0.12)
SOS-RSX-QIDH	1.16(0.96)	0.06(0.06)	2.15(2.02)	0.06(0.06)
ωB2GP-PLYP	0.95(0.94)	0.15(0.15)	1.20(1.20)	0.13(0.13)
SCS-ωB2GP-PLYP	1.41(0.89)	0.16(0.15)	1.91(1.58)	0.13(0.13)
SOS-ωB2GP-PLYP	1.48(0.94)	0.16(0.15)	2.48(2.14)	0.13(0.12)
ωB2PLYP	1.39(1.31)	0.17(0.17)	1.94(1.93)	0.14(0.14)
SOS-ωB2PLYP	1.78(1.05)	0.18(0.17)	2.08(1.65)	0.14(0.14)
ωB88PP86	0.89(0.89)	0.21(0.21)	3.03(3.03)	0.17(0.17)
SCS-ωB88PP86	0.77(0.72)	0.12(0.12)	1.11(1.10)	0.10(0.10)
SOS-ωB88PP86	0.80(0.75)	0.12(0.12)	0.88(0.87)	0.10(0.10)
ωPBEPP86	2.51(2.51)	0.30(0.30)	4.77(4.77)	0.23(0.23)
SCS-ωPBEPP86	0.76(0.76)	0.20(0.20)	1.70(1.70)	0.16(0.16)
SOS-ωPBEPP86	0.73(0.73)	0.19(0.19)	1.08(1.08)	0.15(0.15)

References

(S1) Hancock, A. C.; Goerigk, L. *RSC Adv.* **2023**, *13*, 35964–35984.

(S2) Karton, A.; Martin, J. M. L. *Theor. Chem. Acc.* **2006**, *115*, 330–333.

(S3) Halkier, A.; Jørgensen, P.; Koch, H.; Helgaker, T.; Klopper, W.; Olsen, J.; Wilson, A. K. *Chem. Phys. Lett.* **1998**, *286*, 243–252.

(S4) Neese, F.; Valeev, E. F. *J. Chem. Theory Comput.* **2011**, *7*, 33–43.

(S5) Christiansen, O.; Koch, H.; Jørgensen, P. *J. Chem. Phys.* **1996**, *105*, 1451–1459.

(S6) Hancock, A. C.; Giudici, E.; Goerigk, L. *J. Comput. Chem.* **2024**, *45*, 1667–1681.

(S7) Plasser, F.; Lischka, H. *J. Chem. Theory Comput.* **2012**, *8*, 2777–2789.